Articles   School of Science and Computing

Nanostructured Apatite-Mullite Glass-Ceramics for Enhanced Primary Human Osteoblast Cell Response

Gordon Cooke
Technological University Dublin, gordon.cooke@tudublin.ie

Conor Dunne
UCD, conordnn9@gmail.com

Sarah Keane
UCD

See next page for additional authors

Authors

Gordon Cooke, Conor Dunne, Sarah Keane, Daithi de Faoite, Seamas Donnelly, and Kenneth Stanton

Nanostructured apatite-mullite glass-ceramics for enhanced primary human osteoblast cell response

C.F. Dunne[a], G. Cooke[b], S. Keane[a], D. de Faoite[a],

S.C. Donnelly[c], K.T. Stanton[a],*

[a]UCD School of Mechanical and Materials Engineering, University College Dublin, Ireland

[b]Department of Applied Science, Institute of Technology Tallaght, Ireland

[c]School of Medicine, Trinity College Dublin, Ireland

*Corresponding Author: kenneth.stanton@ucd.ie

Abstract

This work investigates the difference in viability of primary human foetal osteoblast cells on a glass-ceramic surface with nanoscale topography relative to viability on a smooth glass-ceramic surface containing a bioactive phase. Apatite-mullite glass-ceramics containing bioactive fluorapatite ($Ca_{10}(PO_4)_6F_2$) and bioinert mullite ($Si_2Al_6O_{13}$) were synthesised and subsequent heat-treatment was optimised to form nano-sized fluorapatite crystals. Etching was used to selectively remove the bioactive phase, producing a surface with disordered nanoscale topography. Cells were seeded onto a smooth polished glass-ceramic substrate with the bioactive phase intact, an etched nanostructured glass-ceramic with the bioactive phase removed, and a borosilicate glass control. Cell viability after 24 h and 48 h was significantly greater on the nanostructured surface compared to the smooth bioactive surface, while cell viability at both time points was significantly greater on both nanostructured and smooth bioactive surfaces compared to the control.

1   Introduction

The fixation of orthopaedic implants to surrounding tissue can be greatly improved by promotion of osteointegration [1]. The surface chemistry of implants has been shown in many studies to influence osteointegration [2, 3], and bioactive surface coatings such as hydroxyapatite are therefore commonly applied [3]. Apatite-mullite glass-ceramics (AMGCs) are being investigated as an alternative surface coating [4]. AMGCs are triphasic materials composed of fluorapatite ($Ca_{10}(PO_4)_6F_2$) and mullite ($Si_2Al_6O_{13}$) in a residual glass matrix [5]. Fluorapatite is bioactive and promotes cellular attachment [6, 7] and the presence of fluoride ions promotes bone regeneration [8].

Surface topography at the nanoscale has been shown in many studies to significantly influence osteoblast attachment, adhesion, proliferation, and differentiation on a range of biomaterials [9-12]. Nanoscale disordered topographies using polymethylmethacrylate (PMMA) substrates have been shown by Dalby *et al.* to stimulate mesenchymal stem cells (MSCs) to proliferate, differentiate and produce more bone mineral than MSCs seeded onto smooth PMMA substrates [11], demonstrating that surface topography can have significant biological effects.

The crystallisation [13] of AMGCs can be controlled such that only nano-sized fluorapatite crystals are formed. Such AMGCs offer the potential to create nanoscale topography similar to those presented by Dalby *et al.* [11] by selective etching of the fluorapatite phase at the glass-ceramic surface [14]. However, given that fluorapatite is the phase that is typically etched, the topography is produced by removing the bioactive phase from the surface. This provides a novel opportunity to compare the influences of surface chemistry and surface topography on cell viability: the influence surface chemistry can be examined by seeding cells onto an AMGC with the bioactive phase present, with the influence of topography examined by seeding cells onto a disordered nanoscale topography created by removing the bioactive phase.

Immortalised cell lines are widely used in cell culture studies [15]. However, here, for better clinical relevance, primary cells are used.

2   Materials and Methods

A glass with molar composition $4.85SiO_2$–$3.25Al_2O_3$–$1.5P_2O_5$–$3.25CaO$–$1.75CaF_2$, chosen following a review of previous studies [14, 16, 17], was synthesised by melt-quench, as previously described [5, 14]. This composition may produce crystal sizes and spatial density similar to the topographies used by Dalby *et al.* [11]. Some of the glass was re-melted and cast to form cylinders (Ø 11 mm) with annealing at $T_g - 100\,°C$ (560 °C) [14]. Cast cylinders were sectioned into 2.5 mm thick discs.

Glass frit was characterised by differential scanning calorimetry (DSC) [14] to determine the glass transition temperature (T_g) and primary and secondary crystallization peak temperatures (T_{p1} and T_{p2}).

Glass-ceramics were formed by heating glass discs at 10 °C/min to a range of temperatures above T_{p2}, with dwell periods of 0–60 min, followed by cooling in air. Samples were then ground and polished to a sub-micron finish [16].

X-ray diffraction (XRD) was carried out to confirm the amorphous nature of cast glass samples and identify the phases present in heat-treated samples using a Siemens D500 diffractometer (Munich, Germany) with CuKα X-rays from 10°–70° 2θ. Phases were identified using JCPDS-ICDD PDF cards 15-876 (fluorapatite) and 15-776 (mullite).

Glass-ceramic samples were etched for 20 s in 1 M HNO_3, follwed by rinsing in water followed by ethanol and drying. This removes the fluorapatite phase from the surface, leaving the bioinert mullite phase and residual glass.

Microscopical analysis was performed to identify the ideal crystallisation temperature and dwell period for formation a nanostructured surface. Samples were gold sputter coated and imaged using an FEI Quanta 3D FEG-SEM (Eindhoven, The Netherlands). The average pore size and spatial density of pores on substrate surfaces were determined using ImageJ [18].

Three different substrate types were used for cell culturing: a smooth polished AMGC, an etched AMGC, and a borosilicate glass control.

Glass-ceramic samples for cell study were prepared by heat-treating using the ideal crystallisation temperature and dwell period, as determined by microscopical analysis. For sterilisation prior to cell culture, substrates were rinsed in ethanol and distilled water, then covered in aluminium foil and heated to 350 °C for 2 h.

A primary human foetal osteoblast cell line (hFOB 1.19 (ATCC CRL-11372)) was used to assess the biological performance of the substrates. Routine maintenance of the cell line involved culturing in a 1:1 mixture of Ham's F12 Medium and Dulbecco's Modified Eagle's Medium, with 2.5 mM L-glutamine (without phenol red), 0.3 mg/ml G418 and foetal bovine serum to a final concentration of 10 %. Cells were grown at 34 °C, 5 % CO_2, 95 % relative humidity according to ATCC culture guidelines. A sub-cultivation ratio of 1:4 was used with medium renewal every 2–3 days.

Cells were seeded onto the substrate discs (5×10^5 cells/disc) in 24-well plates and cultured for 24 h ($n=5$) and 48 h ($n=6$). Supernatant was then removed and wells with discs were washed with phosphate buffered saline before being placed into new 24-well plates. Cell growth and viability was assessed using WST-1 (Roche Diagnostics, Basel, Switzerland) according to the manufacturer's protocol. WST-1 solution was diluted 1:10 in medium and dispensed into the wells. Plates were incubated for 1 h at 37 °C before absorbance at 440 nm was recorded using a scanning multiwell spectrophotometer (ELISA reader).

Student t-tests were performed to test for statistical significance using P-values ≤ 0.05.

3 Results

DSC analysis of the glass revealed a glass-transition onset at 660 °C, and two crystallisation exotherms, peaking at 790 °C (T_{p1}) and 1016 °C (T_{p2}).

XRD profiles for the as-cast glass and an exemplar glass-ceramic produced by heat-treating to T_{p2} are given in Fig. 1. The profile for the glass exhibits an amorphous halo (17–37° 2θ) with no sharp diffraction peaks, confirming that purely amorphous glass was synthesised and no devitrification occurred during casting. The profile for the glass-ceramic confirms the crystallization of fluorapatite and mullite.
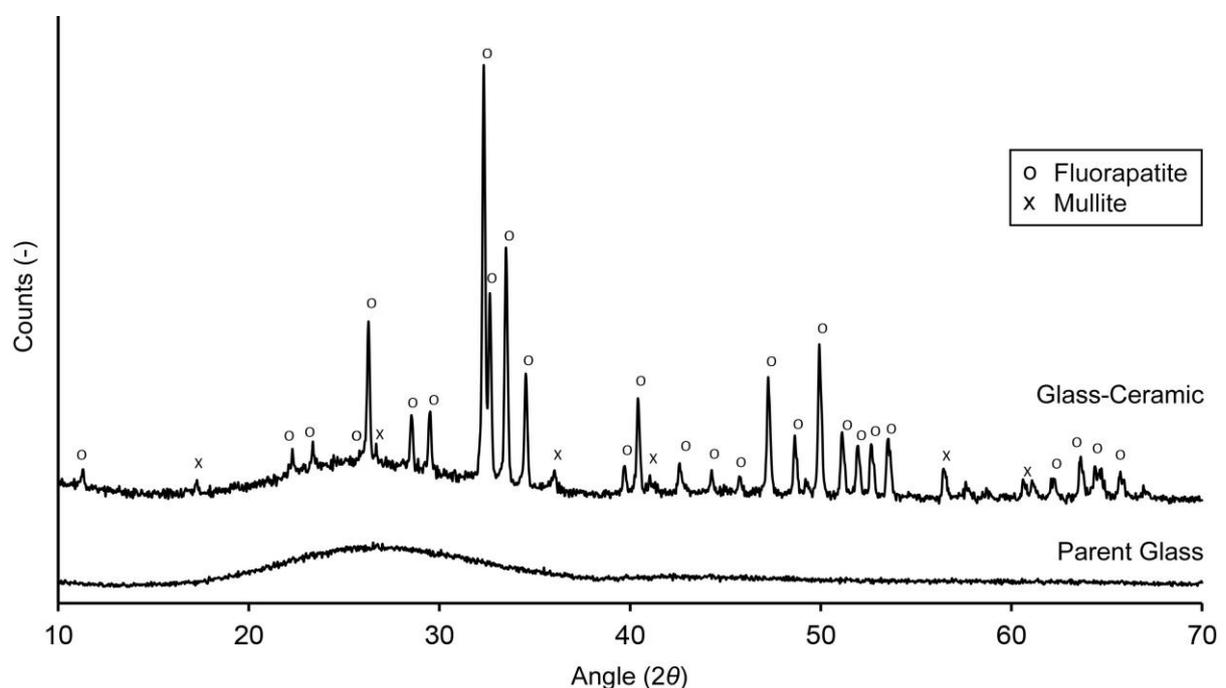

Fig. 1 XRD profiles for as-cast glass and AMGC heat-treated at T_{p2}.

Microscopical analysis revealed that heat-treating to 1100 °C for 20 min produced a glass-ceramic with appropriate nano-sized fluorapatite crystals (Fig. 2). The pores correspond to locations of fluorapatite removed by etching, yielding a disordered nanoscale surface topography. The average pore diameter was 118 ± 53 nm, with a spatial density of ≈ 8 pores/μm^2, approximating the topographies of Dalby *et al.* [11].

Fig. 3 shows the cell viability results. Cells were able to attach to all test surfaces. The smooth and etched AMGC surfaces exhibited significantly better cell viability than the control after 24 h and 48 h ($P < 0.01$). At both time points cell viability was significantly greater on the etched AMGC surfaces compared with the smooth AMGC surfaces ($P < 0.01$).

5
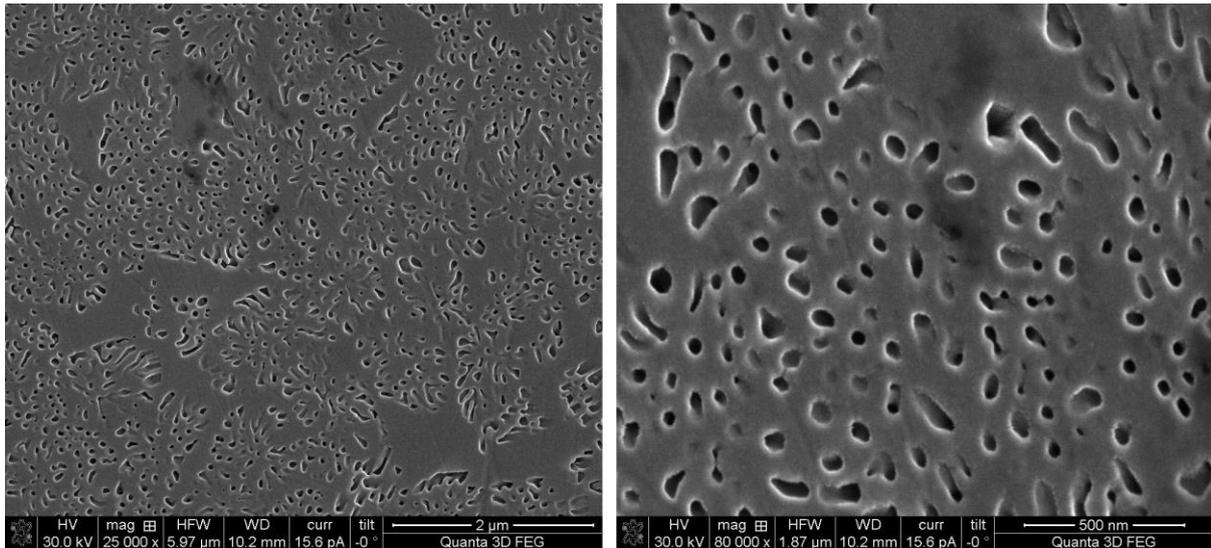
Fig. 2 Micrographs of AMGC heated to 1100 °C for 20 min and etched.
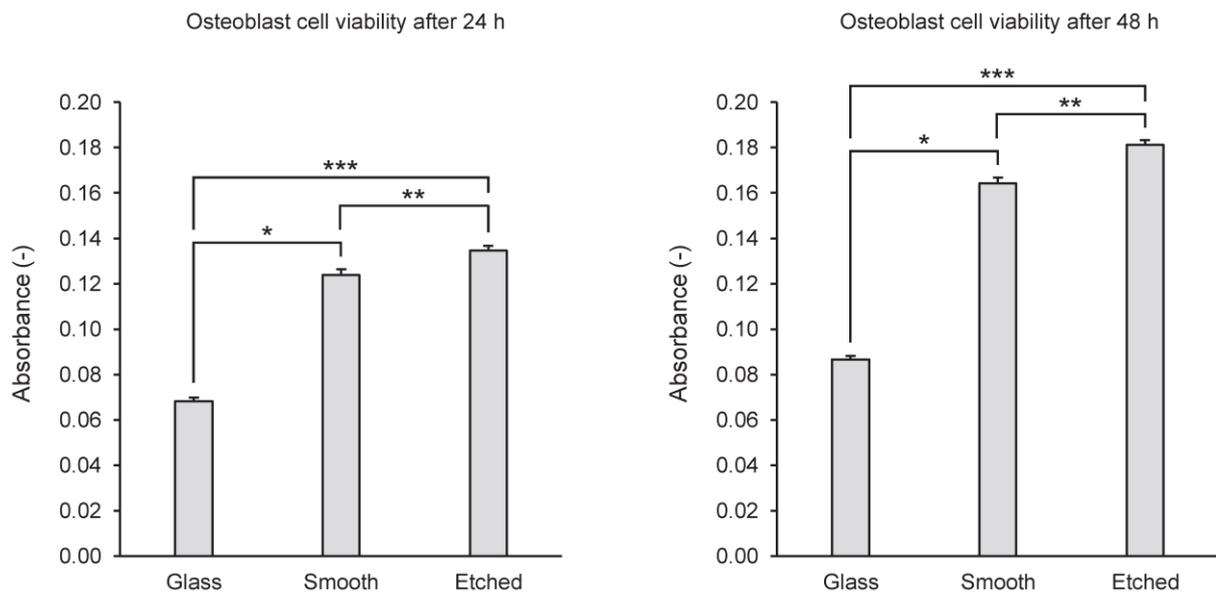
Fig. 3 Optical density measurements for cell viability on test surfaces after 24 h and 48 h.

4 Discussion

After 24 h and 48 h both the smooth and etched surfaces had a significantly greater number of cells present than the control. Etching of the AMGC to remove the fluorapatite phase provided a degree of roughness and an increase in surface area compared to the control. Rough surfaces have been shown to promote cellular attachment by providing more sites for the adsorption of proteins such as fibronectin, which has been shown to promote cellular adhesion [19, 20]. The greater cellular attachment and low toxicity of the etched substrates contributed to the greater cell viability compared to the smooth borosilicate control.

Although the nanostructured substrates exhibited statistically greater cell viability than the smooth AMGC substrates, this difference was relatively low after 24 h (8 %–10 %) and did not increase after 48 h. Given the variability of patient responses and other clinical variables, it would be prudent to not deem this difference *clinically* significant.

5 Conclusion

AMGCs can be used to create disordered nanoscale topographies by controlled heat-treatment and etching of the fluorapatite phase. While these surfaces provide a statistically significant increase in cell viability compared to a smooth bioactive surface, these effects may not produce clinically different outcomes *in vivo*. Expansion of this study to other bioactive glass-ceramics and other cell lines may determine how universal this effect is.

References

[1] Brånemark PI. Osseointegration and its experimental background. Journal of Prosthetic Dentistry. 1983;50:399-410.

[2] Freeman CO, Brook IM, Johnson A, Hatton PV, Hill RG, Stanton KT. Crystallization modifies osteoconductivity in an apatite-mullite glass-ceramic. Journal of Materials Science: Materials in Medicine. 2003;14:985-90.

[3] Buser D, Schenk RK, Steinemann S, Fiorellini JP, Fox CH, Stich H. Influence of surface characteristics on bone integration of titanium implants. A histomorphometric study in miniature pigs. Journal of Biomedical Materials Research. 1991;25:889-902.

[4] Montazerian M, Zanotto ED. Bioactive and inert dental glass-ceramics. Journal of Biomedical Materials Research Part A. 2017;105:619-39.

[5] Stanton K, Hill R. The role of fluorine in the devitrification of $SiO_2 \cdot Al_2O_3 \cdot P_2O_5 \cdot CaO \cdot CaF_2$ glasses. Journal of Materials Science. 2000;35:1911-6.

[6] Qu H, Wei M. The effect of fluoride contents in fluoridated hydroxyapatite on osteoblast behavior. Acta Biomaterialia. 2006;2:113-9.

[7] Hurrell-Gillingham K, Reaney IM, Miller CA, Crawford A, Hatton PV. Devitrification of ionomer glass and its effect on the in vitro biocompatibility of glass-ionomer cements. Biomaterials. 2003;24:3153-60.

[8] Bhadang KA, Gross KA. Influence of fluorapatite on the properties of thermally sprayed hydroxyapatite coatings. Biomaterials. 2004;25:4935-45.

[9] de Oliveira PT, Nanci A. Nanotexturing of titanium-based surfaces upregulates expression of bone sialoprotein and osteopontin by cultured osteogenic cells. Biomaterials. 2004;25:403-13.

[10] Webster TJ, Ergun C, Doremus RH, Siegel RW, Bizios R. Enhanced functions of osteoblasts on nanophase ceramics. Biomaterials. 2000;21:1803-10.

[11] Dalby MJ, Gadegaard N, Tare R, Andar A, Riehle MO, Herzyk P, et al. The control of human mesenchymal cell differentiation using nanoscale symmetry and disorder. Nature Materials. 2007;6:997-1003.

[12] Wang G, Lu Z, Liu X, Zhou X, Ding C, Zreiqat H. Nanostructured glass-ceramic coatings for orthopaedic applications. Journal of the Royal Society Interface. 2011;8:1192-203.

[13] Fokin VM, Zanotto ED, Yuritsyn NS, Schmelzer JWP. Homogeneous crystal nucleation in silicate glasses: A 40 years perspective. Journal of Non-Crystalline Solids. 2006;352:2681-714.

[14] O'Flynn KP, Stanton KT. Nucleation and early stage crystallization of fluorapatite in apatite-mullite glass-ceramics. Crystal Growth & Design. 2010;10:1111-7.

[15] Czekanska EM, Stoddart MJ, Ralphs JR, Richards RG, Hayes JS. A phenotypic comparison of osteoblast cell lines versus human primary osteoblasts for biomaterials testing. Journal of Biomedical Materials Research A. 2014;102:2636-43.

[16] Stanton KT, Hill RG. Crystallisation in apatite-mullite glass-ceramics as a function of fluorine content. Journal of Crystal Growth. 2005;275:e2061-e8.

[17] Stanton KT, O'Flynn KP, Kiernan S, Menuge J, Hill R. Spherulitic crystallization of apatite-mullite glass-ceramics: Mechanisms of formation and implications for fracture properties. Journal of Non-Crystalline Solids. 2010;356:1802-13.

[18] Abramoff MD, Magalhaes PJ, Ram SJ. Image processing with ImageJ. Biophotonics International. 2004;11:36-42.

[19] Martin J, Schwartz Z, Hummert T, Schraub D, Simpson J, Lankford J, et al. Effect of titanium surface roughness on proliferation, differentiation, and protein synthesis of human osteoblast-like cells (MG63). Journal of Biomedical Materials Research. 1995;29:389-401.

[20] Osathanon T, Bespinyowong K, Arksornnukit M, Takahashi H, Pavasant P. Human osteoblast-like cell spreading and proliferation on Ti-6Al-7Nb surfaces of varying roughness. Journal of Oral Science. 2011;53:23-30.